Chapter – II

THEORY AND LITERATURE REVIEW

2.1 Methyl Parathion

Methyl parathion (O,O-dimethyl O-4-nitrophenyl phosphorothioate) was developed in 1940 and first registered as pesticide in 1954 to control insects and pests on a variety of crops. Methyl parathion is also known as dimethyl parathion or parathion-methyl. It is an organo-phosphorous insecticide highly toxic to non-target organisms including humans. It controls boll weevils and many biting or sucking insects of agricultural crops. When methyl parathion is used on the crops, some of it gets dispersed by rain, fog and wind (Memon et al., 2008).

It is a Class I organophosphate insecticide with great concern due to its persistence in the environment, large circulation, and high level of toxicity according to United States Environmental Protection Agency (US EPA 1988; Fan et al., 2011). Methyl parathion contains 16.7% xylene, 80% active ingredient and 3.3% inert ingredients. Primary toxicity mechanism of methyl parathion in nervous system is the inhibition of acetylcholinesterase activity (Dubey et al., 2015). Methyl parathion is synthesized from dimethyl dithiophosphoric acid [$(CH_3O)_2PS_2H$], which is obtained by the treatment of P_2S_5 with methanol. Dimethyl dithiophosphoric acid is chlorinated to generate dithiophosphoryl chloride, which is treated with sodium 4- nitrophenolate (sodium salt of 4- nitrophenol). The reactions are as given below:

$$2(CH_3O)_2P(S)SH + 3Cl_2 \longrightarrow 2(CH_3O)_2P(S)Cl + S_2Cl_2 + 2HCl \quad (2.1)$$

$$(CH_3O)_2P(S)Cl + NaOC_6H_4NO_2 \longrightarrow (CH_3O)_2P(S)OC_6H_4NO_2 + NaCl \quad (2.2)$$

2.1.1 Environmental levels of methyl parathion

2.1.1.1 Air

The minimum concentration level of methyl parathion is not detectable. The maximum level detected was about 70 ng/m^3 (IPCS, 1992).

2.1.1.2 Soil and water

The rate of degradation of methyl parathion depends on temperature and sunlight. It increases with temperature and exposure to sunlight. It has half-life of 1 to 30 days in soil environment and a representative value is estimated to be 5 days (Wauchope et al., 1992). However, the degradation will occur over many years, when higher concentrations of methyl parathion are spread accidentally into the soil, with photolysis being the dominant route. It degrades rapidly in lake, seawater, and river water. 100% degradation will occur in water within 2 weeks to 1 month or more. Degradation of methyl parathion is faster in the presence of sediments and in fresh water than in salt water. Methyl parathion is subject to photolysis in water, with a half-life of 38 days in winter and 8 days during the summer (Howard, 1991).

Fan et al. (2011) reported the highest concentration of parathion in the natural aquatic environment as 0.1 mg/L. In USA, methyl parathion was detected up to 0.46 g/L, with maximum value recorded during the summer (Alves et al., 2013). Muff et al. (2009) investigated methyl parathion concentration of 0.25 mg/L in a dump containing organophosphoric pesticides located nearby the sea in sand dunes.

2.1.1.3 Food

Uptake and metabolism of methyl parathion in plants is fairly rapid. Within 4 days after applying methyl parathion to the leaves of corn, it was almost completely metabolized (Howard, 1991). The surveys conducted in USA (1966 to 1969) indicate that methyl parathion concentrations were highest in root vegetables (up to 1 mg/kg) and leaf

(up to 2 mg/kg) and only few samples of food exceeded the maximum residue limits. The average intake from food found in a survey of USA during 1988 was 0.1 to 0.2 ng/kg of body weight per day (WHO, 2004b).

2.1.2 Toxicity of methyl parathion

Laboratory tests were conducted to observe the effects of methyl parathion on birds and it was found as highly toxic, with lethal concentration (LC_{50}) ranging from 70 to 680 mg/kg diet and lethal dose (LD_{50}) ranging from 3 and 8 mg/kg body weight. It also exhibits highly toxic nature to aquatic invertebrates with LC_{50} ranging from < 1 µg to 40 µg/L (IPCS, 1993). After reviewing the literature on methyl parathion formulations, it was decided that emulsifiable concentrates (EC) with 19.5%, 40%, 50% and 60% active ingredient should be placed in that hazardous category. Active ingredient has generally high toxicity, but several formulations will also fall into a lower category of hazard (FAO, 1989). According to WHO Class I(a) comes in the category of extremely hazardous and Class I(b) in highly hazardous (WHO, 1996). Hazardous classification of methyl parathion formulation is shown in Table 2.1.

Table 2.1: Hazard classification by World Health Organization (WHO, 1996).

Formulation	**Classification of formulations**			
	Oral toxicity		**Dermal toxicity**	
	LD_{50}: 3 mg/kg body weight		**LD_{50}: 40 mg/kg body weight**	
	Active ingredient (%)	**Hazard class**	**Active ingredient (%)**	**Hazard class**
Liquid	>15	Ia	>90	Ia
	1-15	Ib	>5	Ib
	<1	II	1-5	II
Solid	>50	Ia	>40	Ib
	5-50	Ib	3-40	II

2.1.3 Effect of methyl parathion

Methyl parathion (MP) degrades to methyl paraoxon in human body which causes cholinesterase inhibition, overstimulate the nervous system, lead to dizziness, incoordination, headache, sweating, blurred vision, tremor, nausea, tingling sensations, vomiting, abdominal cramps, difficulty in breathing, slow heartbeat and autoimmune disorders (Shriwas and Gogate, 2011; Patil and Gogate, 2012). Very high doses may result in incontinence, unconsciousness, and convulsions or fatality. Its acute toxicity also causes plasma cholinesterase and significant depression of red blood cell but does not cause teratogenic effects. It is nonmutagenic and non carcinogenic (Gallo and Lawryk, 1991).

2.1.4 Guideline values of methyl parathion

Maximum residue limits in food were set at 0.01−0.2 mg/kg. In the workplace, acceptable daily intake is 0.003 mg/kg (FAO, 1996). Accepted daily intake is 0.02 mg/kg body weight in humans. The acceptable concentration of methyl parathion in groundwater is 0.1 µg/L (Council Directive 98/83/EC, Diagne et al., 2007).

2.1.5 Uses of methyl parathion

Food: Methyl parathion has been registered for use on the subsequent crops/sites: alfalfa, peaches, corn, sweet corn, barley, wheat, soybeans, apples, sunflower, and rice fields (Edwards and Tchounwoul, 2005).

Non-food: It is most commonly used on cotton (Edwards and Tchounwoul, 2005).

2.1.6 Reaction pathway of methyl parathion

Degradation of methyl parathion occurs in the presence of water, sunlight, and bacteria found in soil, to other chemical compounds (ATSDR, 2001). The identification of intermediates in the Fenton oxidation of methyl parathion was done with the help of

literature reviewed. The Fenton oxidation of methyl parathion by hydroxyl radicals yields a number of organic intermediates (Evgenidou et al., 2007a).

Methyl parathion isomerizes and hydrolyzes more rapidly. In the environment, methyl parathion quickly oxidizes to more toxic oxon analogue, methyl paraoxon. Methyl paraoxon is generated by the substitution of oxygen for sulphur on the phosphorus atom of methyl parathion as shown in Figure 2.1 (California EPA, 1999). Methyl paraoxon inactivates acetylcholinesterase by phosphorylating the active site of the enzyme and this action further inhibits the hydrolysis of acetylcholine (ATSDR, 2001). The most common by-product of methyl parathion is p-nitrophenol, produced through the hydrolysis of MP and dimethyl phosphorothioic acid. Another possible way to the formation of p-nitrophenol involves the oxidation of methyl parathion to methyl paraoxon and subsequent hydrolysis of methyl paraoxon to p-nitrophenol (Guo and Jans, 2006; Pakala et al., 2007). The important end-products nitrite, sulphate and phosphate formed after methyl parathion degradation can be used as essential nutrients for plants in the agricultural field.

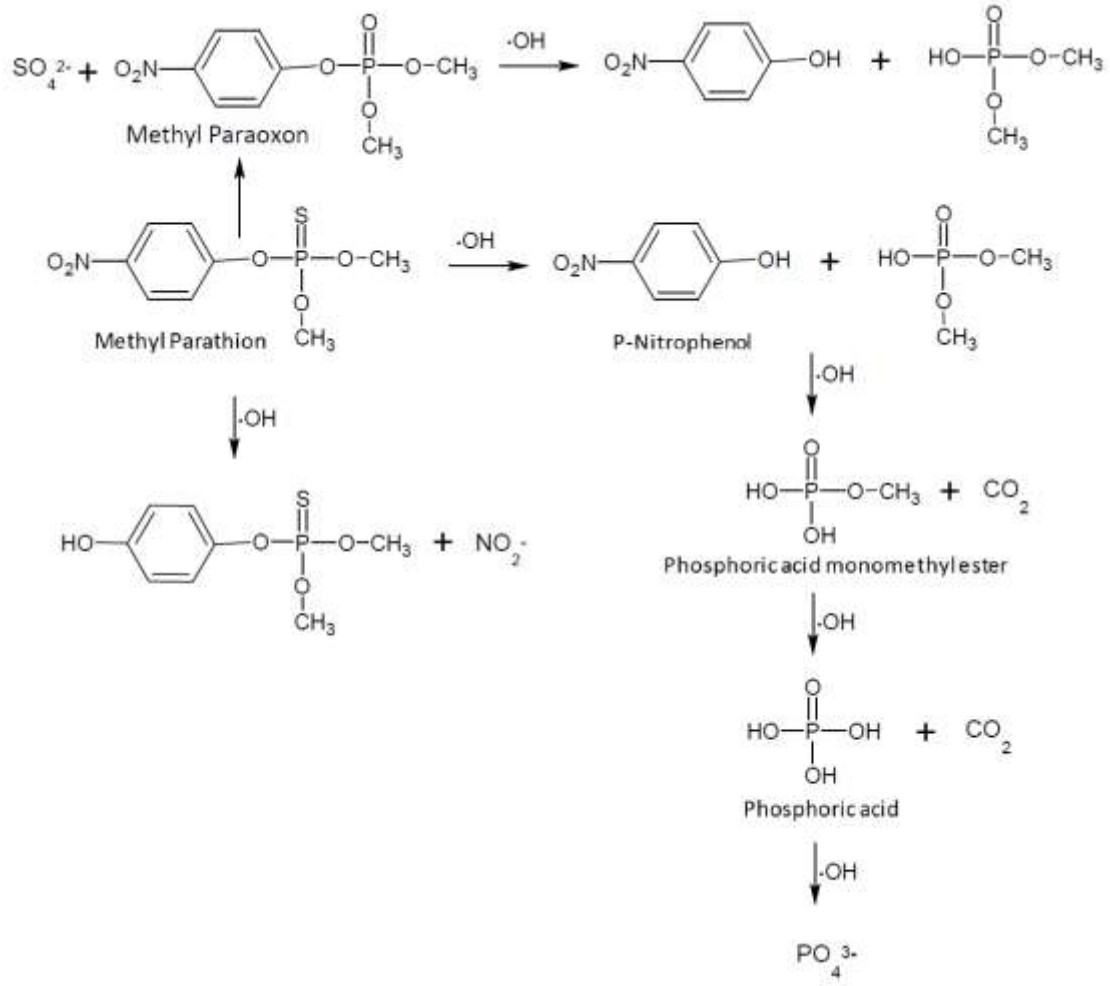

Figure 2.1: Proposed reaction pathway for methyl parathion degradation in Fenton oxidation.

2.1.7 Technologies used for methyl parathion degradation

There have been some reports in the literature on removal of methyl parathion using adsorption, cavitation, photocatalytic degradation, Fenton oxidation, electro-Fenton process, electrochemical oxidation, ultrasonic irradiation and ozonation, etc.

2.1.7.1 Adsorption

Memon et al. (2008) used watermelon peels for the removal of methyl parathion from water using adsorption. They achieved highest adsorption (99±1%) of (0.38–3.80) × 10^{-4} mol dm^{-3} methyl parathion concentration using 0.1 g adsorbent dose, pH 6 and 60 min agitation time. Results showed that with increase in pH, percentage

adsorption was decreased. After 0.1 g of dose, sorption was found constant. With an increase in methyl parathion concentration, the corresponding distribution coefficient (*R*d) decreased. Freundlich adsorption isotherm suggested a better adsorption capacity at lower concentrations of samples rather than higher concentrations. Adsorption kinetics followed first-order rate equation. Thermodynamic analysis indicated endothermic and spontaneous nature of adsorption process.

Akhtar et al. (2007) used rice bran (RB), rice husk (RH), bagasse fly ash (BFA), moringa oleifera pods (MOP) as adsorbent for the removal of methyl parathion from surface and ground water using adsorption. These low cost adsorbents effectively removed 70–90% methyl parathion in 90 min under agitation using 0.1 g adsorbent dose for an initial pesticides concentration of 3.8×10^{-4} M. The Langmuir, Freundlich and Dubinin–Radushkevich (D-R) isotherm models were applied to know the best isotherm. The adsorbent performance was in the order: RB > BFA ~ MOP > RH.

Memon et al. (2007) studied the removal of carbofuran (CF) and methyl parathion (MP) from aqueous solution using chestnut shells as adsorbent. The sorption parameters, i.e., contact time, pH, initial pesticide solution concentration and temperature were studied. Chestnut shells when chemically treated with nitric acid and methanol, significantly increased the sorption capacity of the investigated sorbent. The percentage sorption increased was attributed to the fact that acid treatment of adsorbents dissolved the minerals from the sorbent surface, thereby increasing the pore volume and surface area of the sorbent. The Langmuir, Freundlich and Dubinin–Radushkevich (D-R) isotherms models were applied to know the best fitting isotherm.

A summary on the adsorption studies for the removal of methyl parathion is presented in Table 2.2.

Table 2.2: Methyl parathion removal from contaminated water by adsorption.

Adsorbents	Surface Area	Operating conditions	Optimum conditions	Analysis	Adsorption	Reference
Watermelon peels	Untreated = 15.1 $m^2 g^{-1}$ and treated = 23.4 $m^2 g^{-1}$	Adsorbent dose = 0.05–1 g, Pesticide concentration = (0.38–3.8) × 10^{-4} mol dm^{-3}, Contact time = 10-100 min, pH = 1-10, Temperature = 30 ºC, Agitation speed = 100 rpm	Adsorbent dose = 0.1 g, Contact time = 60 min, pH = 6	HPLC at 240 nm	99±1 %	Memon et al. (2008)
Rice bran, bagasse fly ash, Moringa oleifera pods and rice husk	Rice bran = 28±0.8 $m^2 g^{-1}$, bagasse fly ash = 25±1.5 $m^2 g^{-1}$, Moringa oleifera pods = 27±0.8 $m^2 g^{-1}$ and rice husk = 17±0.6 $m^2 g^{-1}$	Adsorbent dose = 0.025-0.8 g, Pesticide concentration = (0.38–3.8) × 10^{-3} M, Contact time = 10-210 min, pH = 1-10, Temperature = 303±2 K, Agitation speed = 100 rpm	Adsorbent dose = 0.1 g, Pesticide concentration = 3.8×10^{-3} M, Contact time = 90 min, pH = 6, Temperature = 303 K, Agitation speed = 100 rpm	HPLC at 240 nm	70-90 %	Akhtar et al. (2007)
Chestnut Shells	Untreated = 11.6 $m^2 g^{-1}$ and treated = 42 $m^2 g^{-1}$	Adsorbent dose = 0.1-1 g, Pesticide conc = (0.38–3.8)×10^{-4} M, Contact time = 10-100 min, pH =6, Temperature = 373-873 K, Agitation speed = 25-150 rpm	Adsorbent dose = 0.4 g, Pesticide conc = 0.38×10^{-4} M, Contact time = 30 min, Temperature > 573, Agitation speed = 100 rpm	HPLC at 240 nm	Surface water = 99 ± 1 %, Ground water = 99±1.5 %	Memon et al. (2007)

2.1.7.2 Cavitation and sonication

Patil and gogate (2012) examined methyl parathion degradation by hydrodynamic cavitation. Effect of various operating parameters like temperature, pressure and initial pH were evaluated initially. After optimizing the parameters the effect of process escalating parameters like oxidation by Fenton's reagent (H_2O_2:$FeSO_4$ range from 1:1 to 1:6), carbon tetrachloride (1–6 g/L) and hydrogen peroxide at optimum condition were investigated. Authors achieved >90% degradation by combination of hydrodynamic cavitation with H_2O_2 and Fenton's reagent.

Shriwas and Gogate (2011) used low frequency acoustic cavitation (ultrasonic degradation) for degradation of methyl parathion. Effects of presence of CCl_4, H_2O_2 and TiO_2 as additives for escalating the sonodegradation have been inspected. Authors also compared combination of ultrasound generated cavitation with Fenton's chemistry and photocatalysis on degradation process. It was found that addition of additives generated the oxidizing species, which enhanced the sonodegradation process. Authors achieved 99.1% methyl parathion degradation and 75% TOC reduction.

A summary of the studies is given in Table 2.3.

Table 2.3: Methyl parathion removal from contaminated water using cavitation and sonication technique.

Experiment	Operating conditions	Optimum conditions	Analysis	Degradation	Reference
Hydrodynamic cavitation with H_2O_2 and Fenton's reagent	Pesticide concentration = 20-50 ppm, H_2O_2 = 25-200 mg/L, CCl_4 = 1-6 g/L, Temperature = 32, 35 & 39 ºC, pH = 2.2-8.2, Time = 30 min, Inlet pressure = 1-8 bar	Pesticide concentration = 20 ppm, H_2O_2 = 200 mg/L, CCl_4 = 5 g/L Temperature = 39 ºC, pH = 3, Time = 30 min, Inlet pressure = 4 bar	HPLC at 278 nm	MP > 90%, TOC = 76 %	Patil and gogate (2012)
Sonication, Sonication + H_2O_2, Sonication + CCl_4, Sonication + Fenton reaction	Pesticide concentration = 20 ppm, Frequency = 20 kHz, Power = 230 W, TiO_2 = 20-10,000 ppm, H_2O_2 = 60-400 mg/L, CCl_4 = 200-1000 ppm, Temperature = 30 ºC, pH = 2.5-9.3, Time = 60 min	pH = 2.5, Loading of 20:1, 25:1, 10:1 ratio, respectively TiO_2, CCl_4, H_2O_2 to MP concentration	HPLC and UV-VIS-Spectrophotometer at 278 nm	MP = 99.1%, TOC = 75 %	Shriwas and Gogate (2011)

2.1.7.3 Photocatalytic degradation

Senthilnathan and Philip (2011) studied photodegradation of two pesticides, dichlorvos and methyl parathion, by Degussa P-25 TiO_2 and nitrogen (N) doped TiO_2 in a batch reactor under UV, visible and solar light irradiation. They used same pesticides of two types for the analysis - high performance liquid chromatography (HPLC) grade and commercial grade. Different organic compounds such as ethylamine, triethylamine, ammonium hydroxide and urea were used as a source of nitrogen for doping on TiO_2. Under solar radiation N-doped TiO_2 gives better results as compared to UV and visible light. Out of all mentioned nitrogen sources, authors found that N-doped TiO_2 using triethylamine showed better activity under visible and solar light irradiation for methyl parathion degradation. Gas chromatography–mass spectrometry (GC–MS) analysis was preferred to identify by products of both pesticides. In the middle of the process, commercial grade methyl parathion showed O,O-dimethyl phosphonic ester and para-nitrophenol intermediates. In the same way, commercial grade dichlorvos showed O,O,O-trimethyl phosphonic ester and 2,2-dichlorvinyl-O-methyl phosphate intermediates during the reaction.

Wu and Linden (2008) studied photodegradation of parathion by UV and UV/H_2O_2 in aqueous solutions. Direct photolysis of parathion by both low and medium pressure lamps with quantum yields of $6.67 \pm 0.33 \times 10^{-4}$ and $6.00 \pm 1.06 \times 10^{-4}$ mol E^{-1}, respectively was very slow at neutral pH (7). Hydrogen peroxide (H_2O_2) generates hydroxyl radical, which enhanced the photodegradation with a second-order reaction rate constant of $9.70 \pm 0.45 \times 10^{9}$ M^{-1} s^{-1}. An optimum molar ratio of H_2O_2 and parathion was between 300 and 400. Authors also discussed reaction pathways of parathion.

Evgenidou et al. (2007b) used two catalysts TiO_2 and ZnO for degradation of methyl parathion in photodegradation. Authors used Langmuir–Hinshelwood model to describe

degradation kinetics. The results showed a first order kinetics. 100% degradation was attained within 45 and 150 min when treated with TiO_2 and ZnO, respectively. It was reported that initial rate increased linearly up to optimum light absorption with an increase in the amount of catalyst. Rate of photooxidation was enhanced by the addition of an oxidant. It was illustrated that TiO_2 suspensions was more effective in methyl parathion degradation compared to ZnO suspensions.

Moctezuma et al. (2007) used TiO_2 as photocatalyst for degradation of methyl parathion by photodegradation. Four analytical techniques, such as HPLC, ^{1}H NMR, UV–vis and GC–MS were used to identify the intermediate products. Inorganic ions concentration and total organic carbon (TOC) were measured in the reaction. Primary product of degradation was methyl paraoxon under acidic and basic conditions, which eventually degraded to 4-nitrophenol. Under acidic conditions, methyl parathion and its intermediates quickly degraded in a rather fast oxidation process.

Dzyadevych and Chovelon (2002) worked on the degradation of methyl parathion by photodegradation and the toxicity assessments. Primary degradation products (methyl paraoxon and 4-nitrophenol) were examined. The degradation was analyzed by HPLC. Toxicity tests was compared by using a conductometric biosensor based on cholinesterases and a bioassay based on a luminescent bacteria *Vibrio fischeri* (Lumistox).

A summary of the photocatalytic degradation studies is given in Table 2.4.

Table 2.4: Methyl parathion removal from contaminated water by photocatalytic degradation using different catalysts.

Catalyst	Operating conditions	Optimum conditions	Analysis	Degradation	Reference
N-doped TiO_2 and Degussa P-25 TiO_2	Pesticide concentration = 50, 100 and 250 µg/L, Catalysts Concentration = 200 mg/L, Temperature = 25-30 ºC, Time = 90-180 min, Lamp power = 125 W, Lamp wavelength = 340-860 nm, Stirring rate = 150 rpm , Solar radiation = 0-2000W/m^2	Time = 90, 140 & 180 min, solar radiation = 0-1000 W/m^2	GC-ECD,GC-MS	100% under UV light	Senthilnathan and Philip (2011)
Hydrogen peroxide	Pesticide concentration = 10 mM, H_2O_2 Concentration = 0-50 mg/L, Temperature = ambient temperature, Lamp power (medium pressure) = 1 kW, Lamp wavelength = 200-400 nm	Wavelength = 275 nm, H_2O_2 Concentration = 2-10 mg/L	HPLC, GC/EI-MS	90%	Wu and Philip (2008)
TiO_2 and ZnO	Pesticide concentration = 10 mg/L, TiO_2 & ZnO = 10-1000 mg/L, Temperature = 30-35 ºC, Irradiation time = 0-150 min, Lamp power = 125 W, Lamp wavelength = 290 nm	TiO_2 = 200 mg/L, ZnO = 500 mg/L, Time = 150 min	HPLC at 270 nm and GC–MS–EI	1000%	Evgenidou et al. (2007b)
TiO_2	Pesticide concentration = 50 & 300 ppm, Catalysts Concentration = 0.1-0.4 g/100 mL, Temperature = ambient temperature, Time = 3h, Lamp power = 15 W, Lamp wavelength = 365 nm, Time=0-6h, pH = 3-9	Pesticide concentration = 50ppm, Catalysts Concentration = 0.2 g/100 mL, Time = 3h, pH = 3	HPLC at 276 nm, UV-vis, GC-MS and ^{1}HNMR	MP = 95% and TOC = 90%	Moctezuma et al. (2007)
Aactinometry	Pesticide concentration = 10^{-4} M,Temperature = room temperature,Time = 90 min, Lamp power = 125 W	Compared toxicity study	HPLC-PDAD at 270 nm	80%	Dzyadevych and Chovelon (2002)

2.1.7.4 Fenton oxidation

Evgenidou et al. (2007a) selected two insecticides (methyl parathion and dimethoate) for photocatalytic degradation using the photo-assisted Fenton reaction. Different operating conditions such as concentrations of oxidant and iron, temperature and concentration of inorganic ions were selected for degradation kinetics. The replacement of H_2O_2 with peroxydisulfate was also checked. This system attained higher degradation rates. Intermediate products generated during treatment were analyzed using solid-phase extraction (SPE) coupled to a GC–MS unit. The oxidant concentration and ferric ions [Fe^{3+}] varied in the range of 0−100 mg/L and 0.1−6 mg/L, respectively. The luminescent bacteria *V. ficheri* was used for the toxicity analysis. Rate of reaction was increased with increase in ferric ions concentration.

Pignatello and Sun (1995) reported that methyl parathion rapidly decomposed at (1−2) × 10^{-4} M concentration by photoassisted Fenton reaction (Fe^{3+}/H_2O_2/UV). 4-nitrophenol, oxalic acid, O,O-dimethyl-4-nitrophenyl phosphoric acid and dimethyl phosphoric acid were recognised as intermediates. Solutions of ^{14}C-4-nitrophenol evolved CO_2 within 45 min. The outcome of the results recommend that photoassisted Fenton oxidation can be an effective remedy for the treatment of pesticide containing wastewater.

A summary of Fenton and photo-Fenton studies used for removal of methyl parathion is given in Table 2.5.

2.1.7.5 Electro-Fenton process

Diagne et al. (2007) examined methyl parathion degradation by electro-Fenton process in aqueous solutions. Oxidation process generates hydroxyl radicals which leads to mineralization. Experiments were conducted either in nitric acid, sulphuric, perchloric, and hydrochloric media at different pH under current controlled electrolysis conditions.

The effect of pH was also studied on mineralization efficiency in terms of TOC. Degradation intermediates such as inorganic ions, carboxylic acids and aromatic compounds were identified and reaction pathway was proposed. The conditions of this study is summarized in Table 2.6.

Table 2.5: Methyl parathion removal from contaminated water by Fenton and photo-Fenton processes.

Method	Operating conditions	Optimum conditions	Analysis	Degradation	Reference
Photo Fenton	Pesticide concentration = 10 mg/L, H_2O_2 dosage = 0-100 mg/L, Fe^{3+} = 0.1-6 mg/L, Temperature = 15-65 ºC, pH = 2.9, Light intensity = 290 nm, Lamp power = 125 W	H_2O_2 dosage = 40 mg/L, Fe^{3+} = 6 mg/L, Time = 50 min	SPE coupled to GC-MS, HPLC 270 nm	Completely disappeared	Evgenidou et al. (2007a)
Photo Fenton	Pesticide concentration = (1-2) × 10^{-4} M, $Fe(ClO_4)_3$ = 1 × 10^{-3} M H_2O_2 dosage = 10 mM, Temperature = room temperature, pH = 2.8, Light intensity = 300-400 nm	–	LC and either GC/FID or GC/MS	Obsrved by products	Pignatello and Sun (1995)

Table 2.6: Methyl parathion removal from contaminated water by electro-Fenton oxidation.

Anode/ cathode	Electrolyte	Operating conditions	Optimum conditions	Analysis	Degradation	Reference
Carbon felt (17 × 3.5 cm) and Pt	Na_2SO_4, $NaClO_4$, NaCl and $NaNO_3$	Pesticide concentration = 0.13 mM, Temperature = room temperature, Cell voltage = 0.15 V, pH = 1-4, Current density = 60 mA, Time = 0-50 min, Agitation speed = 400 rpm	pH = 3, Time < 50 min	HPLC at 265 nm	TOC = 100%	Diagne et al. (2007)

2.1.7.6 Electrochemical oxidation

Alves et al. (2013) investigated degradation of methyl parathion by electrochemical oxidation in acidic medium under galvanostatic current control using a boron-doped diamond (BDD)/Ti anode. Experiments were conducted in a laboratory-fabricated polypropylene cell containing methyl parathion solution (60 mg/L) at various current densities. HPLC analysis confirmed that 81.2% degradation of methyl parathion was achieved in 180 min at a current density of 100 mA/cm^2 and 4-nitrophenol compound was formed either as a by-product or as an intermediate. Under these conditions maximum TOC reduction observed was 67.6%. Toxicity of the electrolyte was also analysed against the bioluminescent bacterium *Vibrio fischeri* and found that it was reduced considerably.

Mufff et al. (2009) worked on polluted drainage water containing organophosphoric pesticides (methyl-parathion, parathion, ethylaminoparathion, malathion, paraoxon and several phosphoric triesters) from a dump of toxic chemicals waste for degradation by electrochemical oxidation with Ti/Pt90–Ir10 anode, and 316 SS cathode. Process followed a first-order kinetics and COD reduction increased with increase in current density and to a minor extent by increased salinity up to 2.0 w/w%.

Arapoglou et al. (2003) used electrochemical method to detoxify methyl parathion with a Ti/Pt anode and SS 304 as cathode. Electrolysis was performed for 2 hr with sodium chloride (NaCl) as electrolyte. Organic pollutants in the process got wet oxidized to carbon dioxide and water because of the oxidizing potential. Reductions of BOD_5 and COD were both >80% and mean energy consumption was 18–8 kWh per kg^{-1} COD reduced (COD_r). The degradation was more effective in acidic pH of brine solution.

A summary of electrochemical studies used for removal of methyl parathion is given in Table 2.7.

Table 2.7: Methyl parathion removal from contaminated water by electrochemical oxidation.

Anode/ cathode	Electrolyte	Operating conditions	Optimum conditions	Analysis	Degradation	Reference
Boron-doped diamond (BDD)/Ti anode	NaCl	Pesticide concentration = 60 mg/L, Temperature = 25 ºC, Cell voltage = 30 mV s^{-1}, Current density = 5-100 mA cm^{-2}	Current density = 100 mA cm^{-2}	HPLC at 273 nm	MP = 81.2%, TOC = 67.6%	Alves et al. (2013)
Ti/Pt90–Ir10 anode and 316 SS cathode	NaCl	Pesticide concentration = 0.25 mg/L, Temperature = 13 ºC, Cell voltage = 8 to 20 V, pH = 4.2, Current density = 310 to 1131 mA cm^{-2}	Cell voltage = 19 V, Current density = 310 mA cm^{-2}	GC-NPD detector	55 mg/L	Muff et al. (2009)
Ti/Pt anode and SS 304 cathode.	NaCl	Pesticide concentration = 3.6 and 8% (v/v), NaCl = 1-3% (w/v), Cell voltage = 23, 17-18 and 14 V, pH = 2.5-3.3, Current density/Energy consumption = 36 A DC/18-8 kWh per kg^{-1}	Pesticide concentration = 8%, NaCl =1%, pH = 3.3, Energy consumption = 1.642 kWh	–	COD and BOD both >80%	Arapoglou et al. (2003)

2.1.7.7 Ozonation

Usharani et al. (2012) worked on the degradation of methyl parathion (1000 mg/L) by ozonation (batch process) in synthetic solution under variable pH (3 to 9), constant ozone dosage conditions for 120 minutes. The process effectiveness was estimated in terms of COD reduction and methyl parathion conversion. It was detected that alkaline medium is more effective for ozonation. Results showed that pseudo first order rate constant k (1/min) in ozonation was much higher at pH 9 compared to pH 7 and 3. The methyl parathion conversion was observed as 98, 81 and 60% at pH 9, 7 and 3, respectively after 120 minutes and COD reduction was 93% at pH 9. A significant increase in COD reduction was reported at pH > 7.

2.1.7.8 Sonocatalytic degradation

Wang et al. (2007) used two catalysts for degradation of methyl parathion and determined that micron-sized TiO_2 powder had better performance than nano-sized rutile TiO_2 powder. The influences of operating parameters, such as pesticide concentration, the species of TiO_2 particles, TiO_2 amount, ultrasonic intensity, ultrasonic frequency temperature and pH were investigated.

Wang et al. (2006) in another research used nanometer and ordinary anatase titanium dioxide systems in sonocatalytic degradation of organophosphorus insecticide (methyl parathion) and determined that nanometer anatase TiO_2 powder has better performance than ordinary anatase TiO_2 powder. The influence of operating parameters, such as pesticide concentration, the species of TiO_2 catalysts, TiO_2 amount, ultrasonic intensity, ultrasonic frequency temperature and pH were investigated. Degradation kinetics followed a first-order reaction.

The condition of these sonocatalytic degradation studies are summarized in Table 2.8.

Table 2.8: Summary on methyl parathion removal from contaminated water by sonocatalytic degradation in presence of catalysts.

Catalysts	Catalyst size	Operating conditions	Optimum conditions	Analysis	Degradation	Reference
Micron-sized and nano-sized rutile TiO_2 powder	Micron-sized TiO_2=130-150 nm and nano-sized TiO_2=30-50 nm	Pesticide concentration = 25-100 mg L^{-1}, Catalysts concentration = 250-1250 mg L^{-1}, pH = 3-9, Ultrasonic intensity = 20-50 W, Frequency = 20-80 kHz, Temperature = 20-65 ºC, Time = 80 min	Pesticide concentration = 50 mg L^{-1}, Catalysts concentration = 1000 mg L^{-1}, pH = 6.8, Ultrasonic intensities and Frequencies = 50 W and 40 kHz, Temperature = 35 ºC	Micron-sized rutile TiO_2 = 95.6% and nano-sized rutile TiO_2 = 74%	UV–Vis spectra, IC and HPLC at 278 nm	Wang et al. (2007)
Nanometer and ordinary anatase titanium dioxide (TiO_2) powder	Nanometer anatase TiO_2 = 30-50 nm and ordinary anatase TiO_2 = 90-150 nm	Pesticide concentration = 25-100 mg L^{-1}, Catalysts Concentration = 250-1250 mg L^{-1}, pH = 10, Ultrasonic intensity = 0.1-1.0 W cm^{-2}, Frequency = 20-80 kHz, pH=3-9, Temperature = 20-65 ºC, Time = 50 min	Pesticide concentration = 50 mg L^{-1}, Catalysts concentration = 1000 mg L^{-1}, pH = 10, Frequency = 40 kHz, Temperature = 40 ºC, Time = 50 min, Output power = 50W	Nanometer anatase TiO_2 = 96.32% and ordinary anatase TiO_2 = 77.63%	UV–vis spectra and HPLC at 278 nm	Wang et al. (2006)

2.1.7.9 Other techniques

Liao et al. (2016) investigated abiotic degradation (including hydrolysis and oxidation processes) of methyl parathion by α-MnO_2 in batch experiments and found that 90% methyl parathion was decomposed by α-MnO_2 in 30 h. ***Henych et al. (2016)*** prepared titania-iron mixed oxides with various Ti:Fe ratios, and aqueous solutions of titanium(IV) oxysulphate and iron(III) sulphate with urea as a precipitating agent for degradation of methyl parathion. The highest degradation efficiency achieved was <70% at Ti:Fe ratio 0.25:1 and 1:0.25. ***Araujo et al. (2013)*** investigated abiotic degradation of commercially available methyl parathion in simulated solution at two different concentrations (88 mg/L and 200 μg/L). The effect of solar irradiation was evaluated and experimental data showed that photochemical processes were the most efficient in this case. When samples were exposed directly to sunlight, the by-products detected were 4-nitrophenol, methyl paraoxon and *O*,*O*-dimethyl-*O*-*p*hydroxyphenyl phosphorothioate. ***Guo et al. (2006*)** investigated the degradation kinetics of methyl parathion in aqueous solution containing small concentrations of natural organic matter (NOM) and reduced sulfur species from different sources such as river, soil and peat. Experimental data showed that NOM facilitated the transformation of methyl parathion in aqueous solutions containing hydrogen sulphide and followed a pseudo-first-order kinetics.

2.2 Chlorpyrifos

Chlorpyrifos (O, O-diethyl O-3, 5,6-trichloro-2-pyridyl phosphorothioate) is an organophosphate pesticide with moderate toxicity towards mammalians and has a wide diversity on crop and non-crop uses. It has consequential importance because of its wide distribution and is broadly used for controlling pests like white grub, *Holotrichi consanguine*a blanch, which usually affect the groundnut crop. Chlorpyrifos was

introduced in 1965 and registered for use in more than 900 different pesticide formulations worldwide and since then its use has prominently increased. It is used in agriculture for pre- and post- planting soil treatment and household premises (livestock, ornamentals, golf courses, buildings, and wood products) to control pests (Ismail et al., 2013). Chlorpyrifos has been spotted in cord blood, human breast milk, cervical fluid, sperm fluid, and the meconium of newborn infants (EPA, 2000). The level of pesticides in drinking water has become significantly high and is of a big environmental concern. The wastewater bearing chlorpyrifos must be treated as a hazardous waste. In the USA Survey of 2007, chlorpyrifos was reported to rank first among all pesticides (Tiwari and Guha, 2014). It belongs to the phosphorothionate (i.e. phosphorothioate) group and contains P=S substructure. These compounds (in which element =S is replaced by =O) involve metabolic activation for anticholinesterase activity. Chlorpyrifos comes on the fourth place in India, on the basis of consumption pattern after monocrotophos, acephate and endosulfan. The contamination of chlorpyrifos has been found even up to about 24 km from the application field. (Kavitha and Suresh, 2016) and its residues have been detected at an average level of 1.45 mg/kg in eggplant, 0.0662 mg/L in human blood and 0.092 µg/mL in milk samples from buffalo, cow, and female sheep (Nishi and Hundal, 2013).

2.2.1 Environmental levels of chlorpyrifos

2.2.1.1 Air

Concentrations of chlorpyrifos of up to 1428 ng/m^3 have been reported in ambient air in both the gas and particle phases (Munoz et al., 2014).

2.2.1.2 Soil and water

Contamination level of chlorpyrifos in water has been reported to vary from 0.03 µg/L to 15.8 µg/L depending upon the source water (Kabbany et al., 2000;

Banksa et al., 2005). In India, chlorpyrifos has been detected at levels of 4.8 μg/L in soft drinks, which is 47 times higher than the permissible limit recommended by the Bureau of Indian Standards (Ali et al., 2008). Residual chlorpyrifos concentration of the order of 0.003−0.006 μL/L in water samples collected from Kaithal and Pant Nagar areas in India has been reported (Kavitha and Suresh, 2016). Watts (2012) reported the half-life of chlorpyrifos in water of more than 2 months, and in sediment and soil it is more than 6 months. According to another study its half-life in soil is generally 60 to 120 days, but can range from 2 weeks to over 1 year (Lu et al., 2013). Ismail et al. (2013) reported that the half-life of chlorpyrifos, in water at pH 7 and temperature 25 ºC, varied from 35 to 78 days.

2.2.1.3 Food

The residues of chlorpyrifos have been found in a wide range of food stocks, including fruits, vegetables, grains, fish and processed foods. In India it is found in beans, brinjal, cabbage, carrots, cotton, cauliflower, chili, ladyfinger, leeks, mustard, okra, and tomato at up to 0.179 mg/kg mean concentration (Mukherjee, 2003; Ananda and Somashekar, 2012; Sinha et al., 2012).

2.2.2 Toxicity of chlorpyrifos

Chlorpyrifos is the cause of acute toxicity affecting the enzyme acetylcholinesterase in the nervous system. Its oral LD_{50} is 60 mg/kg in rats (Ismail et al., 2013). Toxicity of chlorpyrifos may lead to lung and central nervous system damage, developmental and autoimmune disorders and vomiting.

2.2.3 Effect of chlorpyrifos

Health effects due to chlorpyrifos include myosis, increased urination, diarrhea, diaphoresis, lacrimation and salivation. It is introduced into the body by contact,

ingestion and vapour action. It inhibits the enzyme acetylcholinesterase irreversibly causing convulsions and paralysis (Sharbidre et al., 2011).

2.2.4 Guideline value of chlorpyrifos

The presence of pesticides in drinking water has become significantly high and is a big environmental concern. Numerous studies have reported the maximum detected concentration of chlorpyrifos in ground and surface water as 0−0.3 µg L^{-1} (Tariq et al., 2007), 0.70 µg L^{-1} (Banksa et al., 2005) and 15.8 µg L^{-1} (Kabbany et al., 2000) but WHO recommends MCL of 30 µg/L for drinking water (WHO, 2004a).

2.2.5 Uses of chlorpyrifos

Food: Crops grown with the most intense chlorpyrifos use are rice, corn, tobacco, almonds, beans, maize and fruit trees including oranges, bananas and apples.

Non-food uses: Registered uses include cotton, indoor pest control, mosquito control, termite control, and pet collars (EPA 2000).

2.2.6 Reaction pathway of chlorpyrifos

Chlorpyrifos degraded at slower rates in soils and sediments as compared to aqueous phase. In the aerobic environment (presence of air), chlorpyrifos can either hydrolyze to diethylthiophosphate (DETP) and 3,5,6- trichloro-2-pyridinol (TCP) or degraded to chlorpyrifos oxon (CPFO) and subsequent hydrolysis to TCP and diethylphosphate (DEP) in the presence of hydroxyl radicals (Silambarasan and Abraham, 2013; Samet et al., 2010a). TCP is further broken down to trichloro-methoxypyridine (TMP) and smaller products such as CO_2, NH_4^+, CO_3^{2-}, NaCl, aliphatic amine and carboxyl compounds (Serrano et al., 1997; Tiwari and Guha, 2014). DETP is further metabolized to ethanol and phosphorothioic acid. According to Tiwari and Guha (2014) the most toxic intermediate in the pathway, CPFO was not identified in anaerobic environment,

was short lived in aerobic environment and in aqueous medium, but accumulated slowly in the soils. Figure 2.2 represents the chlorpyrifos degradation in aqueous phase.

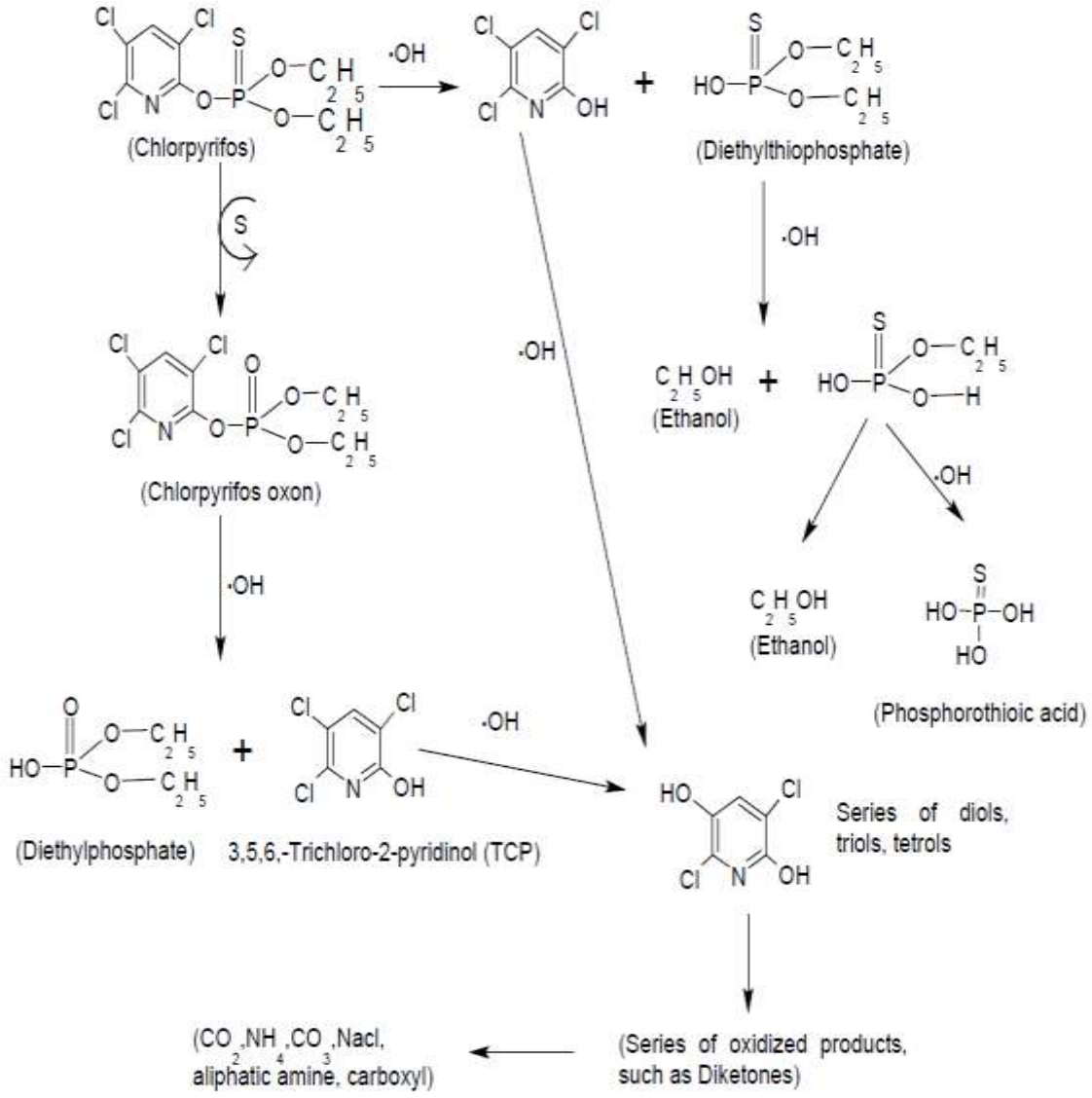

Figure 2.2: Proposed reaction pathway for chlorpyrifos degradation in aqueous phase.

2.2.7 Technologies used for chlorpyrifos degradation

Available results on degradation of chlorpyrifos using irradiation process, biodegradation, Fenton, photo-Fenton, photocatalytic degradation and electrocoagulation/electrochemical method are discussed in following sections.

2.2.7.1 Irradiation process

Ismail et al. (2013) studied the irradiation of chlorpyrifos using a 60Co γ-rays source. Irradiation process showed 100% degradation at 500 µg/L concentration with dose rate of 300 Gy/h at an absorbed dose of 575 Gy. The chlorpyrifos radiolysis decay follows pseudo-first order process with respect to dose. The effect of saturated solutions of N_2O and N_2, and radical scavengers iso-propanol, tert-butanol, H_2O_2, $NaNO_2$ and $NaNO_3$ on the degradation of chlorpyrifos were also observed. The inorganic byproducts after degradation were quantified in terms of Cl^-, SO_4^{2-} and PO_4^{3-} by IC.

Hossain et al. (2013) studied the degradation of chlorpyrifos using gamma irradiation and sunlight. Different concentrations of chlorpyrifos were irradiated wih 1–10 kGy in distilled water. Lower concentration (< 5 mg/L) gave higher removal as compared to higher concentrations (10 and 20 mg/L). The degradation of chlorpyrifos by sunlight in lake water was 51.95%, whereas in distilled water was 39.5% in 12 days. The highest degradation rate was obtained in lake water in one day as 7.4% per day at the light intensity of 42, 200 lx and in distilled water in nine days (4.2% per day) at the light intensity of 43, 400 lx. Summary of the results of irradiation processes used for the removal of chlorpyrifos is given in Table 2.9.

Table 2.9: Chlorpyrifos removal from contaminated water using Irradiation technique.

Irradiation source	Operating conditions	Operating conditions	Analysis	Degradation	Reference
Cobalt-60 gamma irradiation source	Chlorpyrifos concentration = 200–1000 µg L^{-1}, Gamma radiation dose = 30–575 Gy, Temperature = 22 ºC, H_2O_2 = 4 mM or 50 mM	Chlorpyrifos concentration = 500 µg L^{-1}, Gamma radiation dose = 575 Gy, Dose rate = 300 Gy h^{-1}, H_2O_2 = 4 mM	IC, SPME–GC–ECD	100%	Ismail et al. (2013)
Cobalt-60 gamma irradiation source and natural sunlight	Chlorpyrifos concentration = 5-20 mg/L, Gamma radiation dose = 1-10 kGy, Study period = 12 days, Temperature = 30 ºC	Chlorpyrifos concentration = 5 mg/L, Gamma radiation dose = 1.5-5.6 kGy, Dose rate = 4.79 kGy h^{-1}	HPLC with Photo Diode Array (PDA) detector	> 85%	Hossain et al. (2013)

2.2.7.2 Biodegradation

Pailan et al. (2016) used *Acinetobacter sp.* to degrade chlorpyrifos in soil and found that strain could degrade 98% chlorpyrifos within 144 h. Thin layer chromatography (TLC), HPLC and GC-MS were used to identify the intermediate products. Analyses revealed that 3,5,6 trichloro-2-pyridinol (TCP) was recognized as the only major intermediate during degradation process.

Tiwari and Guha (2014) investigated the reduction of chlorpyrifos in aqueous and soil slurry (1:3 w/w) media by the enriched indigenous soil microorganism for 15 days in aerobic and 60 days in anaerobic batch scale processes. At the end of the experiments, 2.78 ± 0.11 mM of chlorpyrifos was degraded by 66% in aqueous anaerobic and 82% in aerobic conditions, while 12.4 ± 0.5 mM of chlorpyrifos was degraded by 31% under anaerobic and 48% under aerobic soil slurries. The degradation of chlorpyrifos in soil

slurries was slower (2-10 times) than water. Authors also performed biodegradation experiments using market grade chlorpyrifos (20% emulsified concentrate, Radar; ISAGRO ASIA, India) acquired from the local market.

Yadav et al. (2014) investigated biodegradation of chlorpyrifos by *Pseudomonas* (Iso 1) sp. in batch as well as continuous bioreactors. The optimum condition in batch experiments for maximum removal were: chlorpyrifos concentration 500 mg/L; inoculum level 300 × 10^6 Cfu/mL; pH 7.5; dissolved oxygen (DO) 5.5 mg/L and temperature 37 ºC. The continuous bioreactor (packed bed) was operated at flow rates 10–40 mL/h, under the optimum conditions. Removal efficiency of chlorpyrifos was observed more than 91% up to the inlet load of 300 mg/L/d.

El-Helow et al. (2013) used bacterial strain, *B. subtilis* Y242 for degradation of chlorpyrifos and observed that this bacterial strain degraded 95.12% chlorpyrifos of 150 mg/L within 48 h. Degradation was examined by GC-MS and HPLC.

Lu et al. (2013) used bacterial strain, *Cupriavidus sp*. DT-1, to degraded chlorpyrifos and 3,5,6-trichloro-2-pyridinol (TCP). Degradation pathway of chlorpyrifos was also investigated. Inoculation of chlorpyrifos-contaminated soil with strain *Cupriavidus sp*. DT-1 obtained 100% and 94.3% degradation rate of chlorpyrifos and TCP, respectively as compared to 28.2% and 19.9% degradation rate in uninoculated soil.

Silambarasan and Abraham (2013) studied degradation of chlorpyrifos with nutrients and also in absence of nutrients using *Alcaligenes sp.* JAS1 bacterial strain. The isolated bacterial strain degraded 300 mg/L of chlorpyrifos in 12 h of incubation and 3,5,6-trichloro-2-pyridinol (TCP) was observed as an intermediates in the aqueous medium. In study of soil sample with and without nutrients along with chlorpyrifos and JAS1 bacterial strain showed complete chlorpyrifos degradation in 24 h and 48 h,

respectively. Kinetic studies showed that degradation followed first and pseudo first order models. Biodegradation of TCP in aqueous medium by *Alcaligenes sp.* JAS1 reduced by 50% in 0.5 d. In study of TCP degradation in soil sample with and without nutrients along JAS1 bacterial strain showed 50 % TCP degradation in 0.6 d and 0.7 d, respectively.

Farhan et al. (2012) isolated 35 microbial strains from effluents of chlorpyrifos manufacturing plant. All strains have different ability for chlorpyrifos degradation and resistance against it. Among these one strain (WW5) was found effective in chlorpyrifos degradation and most resistant. On the basis of characterization i.e. morphological, biochemical and physiological, it was identified as *Pseudomonas sp.* bacterial strain. Biodegradation study at various operating conditions using WW5 strain was conducted and 94% chlorpyrifos (400 mg/L) degradation was obtained at efficient results pH 8, inoculum density (108 Cfu/mL) and 18 days of incubation.

Maya et al. (2012) used fungal isolates from soil for the degradation of chlorpyrifos and TCP. The biodegradation of chlorpyrifos and TCP showed 69.4 to 89.8% and 62.2 to 92.6% degradation, respectively, after one week. Fungal bacterial strains showed high affinity for chlorpyrifos and TCP. The genetic affinity of isolate F1 to *Aspergillus sp.*, F2 and F3 to *Penicillium sp.*, F4 to *Eurotium sp.* and F5 to *Emericella sp.* were confirmed. The degradation efficiency was in the order: F1 > F2 = F3 > F4 > F5.

Vijayalakshmi and Usha (2012) isolated *Pseudomonas putida* from an agricultural soil for the degradation of chlorpyrifos in both free and immobilized situations. Free cells of *Pseudomonas putida* showed 76% degradation at pH 7, 2% chlorpyrifos concentration, temperature 35 °C, agitation speed (150 rpm), inoculum size (10 mL), and in presence of 300 mg/L yeast extract and 200 mg/L glucose. When Ca-alginate immobilized cells were used for chlorpyrifos, 96% degradation was achieved at 2% chlorpyrifos

concentration. On increasing the pesticide concentration to 10%, both free cells and immobilized cells showed 43 and 63%, degradation, respectively. Experimental results showed immobilized cells provide better efficiencies compared to free cells.

A summary of the results of biodegradation studies is given in Table 2.10.

Table 2.10: Chlorpyrifos removal from contaminated water by bacterial strain using biodegradation.

Bacterial strain	Experiment setup	Sample	Operating conditions	Analysis	Degradation	Reference
Acinetobacter sp. strain MemCl4	Flasks	Soil	Chlorpyrifos concentration = 250 µg/mL, Inoculum level = 50-1250 µg/mL, pH = 6.8, Temperature = 26 ºC, Time = 24 h	TLC, HPLC at 290 nm and GC-MS	98%	Pailan et al. (2016)
Nutrient Agar for aerobic and Anaerobic Agar for anaerobic exp.	Borosilicate glass vials	Aqueous and soil slurry	Chlorpyrifos concentration = 2.78 ± 0.11 mM, Inoculum level = Aerobic 3.35 ± 0.07 and anaerobic 4.60 ± 0.21 mg/L , pH = Soil 7.9-8.2, Temperature = 18-31 ºC, avg. 25 ºC, Time = 15 d for aerobic and 60 d for anaerobic	GC-MS/MS	82% in aerobic and 66% in anaerobic aqueous environments	Tiwari and Guha (2014)
Pseudomonas sp.	Continuous packed bed bioreactor	Soil	Chlorpyrifos concentration = 100-700 mg/L, Inoculum level = 50-500 $\times 10^6$ cell mL^{-1}, pH = 6.9, Temperature = 25-45 ºC, DO = 3.2-7.8 mg/L	HPLC at 214 nm	> 91%	Yadav et al. (2014)
Bacillus subtilis Strain, Y242	Petri dish	Water samples from agricultural wastewater	Chlorpyrifos concentration = 150 mg/L, Inoculum level = 10^9 Cfu/mL, pH = 8, Temperature = 30 ºC, Time = 48 h	GC-MS and HPLC	95.12%	El-Helow et al. (2013)

Cupriavidus sp. DT-1	Glass beaker	Soil	Chlorpyrifos concentration= 100 mg/L, Inoculum level = 2×10^6 Cfu mL^{-1}, pH = 7, Temperature = 30 ºC, Time = 6 h	HPLC at 230 nm	100%	Lu et al. (2013)
Alcaligenes sp. JAS1	Shake flask at 120 rpm	Soil and aqueous medium	Chlorpyrifos concentration = 100-300 mg/L, Inoculum level = 3×10^6 cells mL-1, pH = 6.8-7, Temperature = 30 ± 2 ºC, Time = 5 days	HPLC at 230 nm	MSM 98.6±1.3, soil 95.2±3.4%	Silambarasan and Abraham (2013)
Pseudomonas sp.	Shake flask at 100 rpm	Soil	Chlorpyrifos concentration = 100-600 mg/L, Inoculum level = (10^3-10^8) Cfu mL^{-1}, pH = 6.8-5, Temperature = 37 ºC, Time = 18 days	HPLC at 290 nm	94%	Farhan et al. (2012)
Fungal isolates	Shake flask at 150 rpm	Soil	Chlorpyrifos concentration= 25-200 mg/L, pH = 7.2, Temperature = 28ºC, Time = 7 days	HPLC at 214 nm	69.4 to 89.8%	Maya et al. (2012)
Cladosporium cladosporioides strain Hu-01	Glass beaker	Water	Chlorpyrifos concentration = 50 mg/L, pH = 3.97-9.02, Temperature = 26.8 ºC, Time = 12 h	GC-MS, HPLC with array detection from 190–400 nm	85 %	Chen et al. (2012)
Free and immobilized cells of *Pseudomonas putida*	Flasks	Water	Chlorpyrifos concentration = 2-10%, Inoculum level = Free cells: 4×10^2 Cfu mL^{-1}, Immobilized cells: 5×10^2 Cfu/bead, pH = 7, Temperature = 37 ºC, Time = 24 h	Spectrophotometric at 520 nm	Free cells: 76%, Immobilized cells:96%	Vijayalakshmi and Usha (2012)

Acremonium sp. strain (GFRC-1)	Erlenmeyer flask	Soil	Chlorpyrifos concentration = 300 mg/L, Inoculum level = 0.1 mL, pH = 8.10, 6.64 & 7.50 of 3 soil, Temperature = 30 ± 2 ºC, Time = 72 h	LC-MS	83.9%	Kulshrestha and Kumari (2011)
Spirulina platensis ARM728	Glass beaker	Water	Chlorpyrifos concentration = 10-120 ppm, pH = 7, Temperature = 28 ºC, Time = 1 h	HPLC at 230 nm	87%	Thengodkar and Sivakami (2010)
Verticillium sp. DSP	Flasks at 150 rpm	Soil	Chlorpyrifos concentration = 1-500 mg/L, Inoculum level = 2.5 g (wet weight)/L, pH = 5, 7 & 9, Temperature = 15-35 ºC, Time = 2 h-25 days	GC-FPD	Half-lives shortened by 12.0% (greenhouse) and 37.1% (open field) in inoculated soils	Fang et al. (2008)

2.2.7.3 Fenton and photo-Fenton

Affam et al. (2016) treated three pesticides chlorpyrifos, chlorothalonil and cypermethrin in aqueous solution by the FeGAC/H_2O_2 process. At optimum conditions (pH 3, FeGAC dose 5 g/L and H_2O_2 concentration 100 mg/L), chemical oxygen demand (COD) and total organic carbon (TOC) removals were obtained as 96.2 and 79.2%, respectively, and biodegradability of chlorpyrifos (BOD_5/COD ratio) got improved from 0 to 0.40 after reaction time of 60 min. Complete degradation (100%) of chlorpyrifos, chlorothalonil and cypermethrin pesticides active ingredients occurred in 1 min.

Affam et al. (2014) treated pesticide wastewater (Malaysian industrial effluent) containing chlorpyrifos, chlorothalonil and cypermethrin, to meet discharge standards, using UV Fenton pretreatment combined with aerobic sequencing batch reactor. At optimum conditions in the pretreatment phase (pH 3, H_2O_2/Fe^{2+} molar ratio 25, H_2O_2/COD molar ratio 2.0, and reaction time 60 min), biodegradability of chlorpyrifos (BOD_5/COD ratio) increased from 0.02 to 0.31 after reaction time of 60 min. In the UV Fenton-SBR process maximum COD and TOC removal were achieved after 40 day operation at 12 h HRT.

Alalm and Tawfik (2013) presented comparison study between the performance of Fenton (Fe^{2+}/H_2O_2) and photo-Fenton ($TiO_2/Fe^{2+}/H_2O_2$/UV) processes for chloropyrifos (200 mg/L), and COD removal from pesticide wastewater collected from agrochemical and pesticides company located in Nubaria, Egypt. Both processes were very effective for removal of chloropyrifos and COD at an optimum dosage of 1 gm/L H_2O_2, 4 gm/L $FeSO_4.7H_2O$ and 2 gm/L TiO_2. However, the removal efficiency improved by 27% with photo catalytic oxidation process as compared to Fenton oxidation.

Samet et al. (2012) compared Fenton (H_2O_2/Fe^{2+}) and solar photo-Fenton process (H_2O_2/Fe^{2+}/solar light) for chloropyrifos removal. Overall degradation kinetics was defined by a pseudo-second-order rate equation with respect to COD. The optimum process conditions were obtained at the initial COD 1330 mg/L, pH 3, $[Fe^{2+}]_0$ 5.0 mM, H_2O_2 dosing rate 120 $mg \cdot min^{-1}$ and temperature 35 °C for the Fenton oxidation. However, to attain 90% of COD removal, Fenton process needed 50% more time than solar photo-Fenton process.

A summary of the Fenton and photo-Fenton studies is presented in Table 2.11.

Table 2.11: Chlorpyrifos removal from contaminated water by Fenton and photo-Fenton process.

Method	Operating conditions	Optimum conditions	Degradation	Analysis	Reference
FeGAC/H_2O_2 process	Pesticides concentration = 400 mg/L of the pesticides (100 mg/L of chlorpyrifos, 50 mg/L of cypermethrin and 250 mg/L of chlorothalonil), H_2O_2 dosage = 10-300 mg/L, FeGAC = 1-5 g/L, pH = 2-8, Time = 60 min	H_2O_2 dosage = 100 mg/L, FeGAC = 5 g/L, pH = 3	COD = 96.2%, TOC = 79.2%, biodegradability (BOD_5/COD ratio) increased from 0 to 0.40	HPLC at 230 nm	Affam et al., (2016)
UV Fenton and sequencing batch reactor (SBR)	Chlorpyrifos concentration = 805.56±10.0 mg/L, H_2O_2 dosage = 157-366.4 mM, Fe^{2+} = 2.09 and 41.8 mM, Temperature = 25±2 ºC, pH = 3, Light intensity = 6 W, emitting radiation at ~365 nm	H_2O_2/COD molar ratio 2.0, H_2O_2/Fe^{2+} molar ratio 25	Overall by UV Fenton-SBR: COD = 96.2%, TOC = 97.4%	GC-MS	Affam et al. (2014)
Fenton and photo-Fenton ($UV/Fe^{2+}/H_2O_2$) and TiO_2 assisted photo-Fenton ($UV/TiO_2/Fe^{2+}/H_2O_2$)	Chlorpyrifos concentration = 200 mg/L (Industrial wastewater), H_2O_2 = 0-2 g/L, TiO_2 = 0-2 gm/L,Fe^{2+} = 1-5 g/L, pH = 2.5-11.4, Time = 0-60 min (Fenton) & 0-180 min (photo-Fenton), Light intensity = 300 W/m^2	H_2O_2 dosage = 1 g/L, TiO_2 = 2 gm/L, Fe dosage = 4 g/L, pH = 3.6, Time = 45 min (Fenton) & 120 min (photo-Fenton)	Fenton: COD = 86%, chlorpyrifos = 61.8%; Photo-Fenton: COD = 91%, chlorpyrifos = 78%;	HPLC at 300 nm	Alalm and Tawfik (2013)
Fenton and photo-Fenton ($UV/Fe^{2+}/H_2O_2$)	COD_0 = 465, 825 and 1330 mg/L, H_2O_2 dosage = 30-180 mg/min, Fe dosage = 0.5-8.0 mM, Temperature = 20-45 ºC, pH = 2.5-4, Time = 0-70 min, Light intensity = 850 W/m^2	COD_0 = 1330 mg/L, H_2O_2 dosage = 120 mg/min, Fe dosage = 5 mM, Temperature = 35 ºC, 20-45 ºC, pH = 2.5-4, Time = 70 min	COD = 90%	UV/Vis Spectrophotometer	Samet et al. (2012)

2.2.7.4 Photocatalytic degradation

Amalraj and Pius (2015) performed photocatalytic degradation of monocrotophos (MCP) and chlorpyrifos using TiO_2 catalyst irradiated with 16 W UV light source. The effect of various operating parameters, i.e. pesticide concentration, photocatalyst concentration, and pH on the percentage degradation were studied. The kinetics of both pesticides followed Langmuir–Hinshelwood model, under different initial concentration.

Affam and Chaudhuri (2013) performed photocatalytic degradation of chlorpyrifos, chlorothalonil and cypermethrin in aqueous solution using TiO_2 as photocatalyst under UVA (365 nm) irradiation. In UV/TiO_2 photocatalysis process TOC and COD removal were 8.45 and 25.95%, respectively. In UV/TiO_2/H_2O_2 photocatalysis process TOC and COD removal were 21.54 and 53.62%, respectively and biodegradability index increased to 0.26. UV/TiO_2/H_2O_2 photocatalysis process was more effective in degradation of pesticides in aqueous solution. Photocatalytic degradation followed pseudo-first order kinetics.

Muhamad (2010) studied photocatalytic degradation of chlorpyrifos (5 mg/L) in different types of natural water such as river, lake, ground as well as in drinking and distilled water under simulated irradiation sources and natural sun light. Kinetic experiments were examined using HPLC connected with UV-detector. The photo-degradation followed pseudo-first-order kinetics. The TiO_2/UV gave high process efficiency compared to the TiO_2/visible or TiO_2/sun processes. Photocatalytic degradation rate followed the following order: distilled water >ground water > lake water >river water > drinking water.

A summary of results of photocatalytic degradation for chlorpyrifos removal is presented in Table 2.12.

Table 2.12: Chlorpyrifos removal from contaminated water using photocatalytic degradation in presence of catalyst.

Catalyst	Operating conditions	Optimum conditions	Analysis	Degradation	Reference
TiO_2	Chlorpyrifos concentration= 2-10 mg/L, TiO_2 concentration = 0.2-1.4 g/L, Temperature = 25-30 ºC, Time = 10-80 min, pH = 1-13, Light intensity = 252 nm, Lamp = 16 W UV light source	Chlorpyrifos concentration = 2 mg/L, TiO_2 concentration = 1 g/L, Temperature = 25-30 ºC, Time = 60 min, pH = 5	UV–vis spectrometer at 450 nm	98%	Amalraj and Pius (2015)
TiO_2/H_2O_2	Pesticide concentration = 400 mg/L of the pesticides (100 mg/L of chlorpyrifos, 50 mg/L of cypermethrin and 250 mg/L of chlorothalonil), TiO_2 = 0.5-2.5 g/L, H_2O_2 = 50-300 mg/L, Temperature = 23±2 ºC, Time = 300 min, Light intensity = 365 nm, Lamp = 6W	TiO_2 = 1.5 g/L, H_2O_2 = 100 mg/L, Temperature = 23±2 ºC, Time = 300 min, pH = 6	GC-MS	COD = 53.62%, TOC = 21.54%	Affam and Chaudhuri (2013)
TiO_2	Chlorpyrifos concentration = 5 mg/L, TiO_2 concentration= 0.02-0.15 g/L, Temperature = 30 ºC, Time = 0-400 min, Light intensity = 603-729 Wm^{-2}, Solar radiation = 285-2800 nm, Lamp = Tungsten lamp 500 W	Chlorpyrifos concentration = 5 mg/L, TiO_2 concentration= 0.2 g/L, Time = 150 min	HPLC at 228 nm	Distilled water >ground water > lake water >river water > drinking water	Muhamad (2010)

2.2.7.5 Electrocoagulation method

Abdel-Gawad et al. (2012) used electrocoagulation method for the removal of three pesticides (malathion, chlorpyrifos and imidacloprid). The percentage removal of all the three pesticides were ~ 98−99%, when iron was used as a sacrificial anode under various operating conditions.

Robles-Molina et al. (2012) investigated electrochemical transformation of chlorpyrifos in wastewater. The electrochemical oxidation was carried out in a batch mode, using diamond-based material as anode and stainless steel as cathode. Experiment was conducted at two different concentrations (1.0 mg/L and 0.1 mg/L). The outcomes of results showed completely degradation of chlorpyrifos at the end of reaction time.

Samet et al. (2010a) used electrochemical process for the total mineralization of water contaminated with pesticides like chlorpyrifos. The process was carried out using Nb/PbO_2 anodes and graphite carbon bar as cathode. The mineralization efficiency was evaluated in terms of COD measurement and the process followed the pseudo second-order kinetics. The maximum COD removal (76%) was obtained at apparent current density 50 mA/cm^2, temperature 70 ºC, initial COD = 450 mg/L and 10 h electrolysis time.

Samet et al. (2010b) investigated electrochemical transformation of chlorpyrifos in aqueous solutions. The electrochemical oxidation was carried out using boron-doped diamond (BDD) as anodes and graphite carbon bar as cathode. The mineralization efficiency was evaluated in terms of COD measurement and process followed the pseudo first-order kinetics. The complete degradation (100%) was obtained at applied current density 20 mA/cm^2, temperature 70 ºC, initial COD = 456 mg/L and 6 h electrolysis time.

A summary of the results of electrocoagulation process for chlorpyrifos degradation is presented in Table 2.13.

Table 2.13: Chlorpyrifos removal from contaminated water by electrochemical process.

Anode and cathode	Operating conditions	Electrolyte	Analysis	Degradati-on	Reference
Iron cathode and anode	Chlorpyrifos concentration = 0.5%, Temperature = 25 ºC, pH = 1-10, Electrolysis time = 10 min, Stirring intensity = 100 rpm, Cell voltage = 0-15 V, Current density and Energy consumption = 1 mA/cm^2 and 1.5 kwh/kg	NaCl (1 g/L)	–	COD = 98-99%	Abdel-Gawad et al. (2012)
Diamond-based material anode and stainless steel (AISI 304) cathode	Chlorpyrifos concentration = 0.1-1.0 mg/L, Temperature = 25 ºC, pH = 1-10, Electrolysis time = 10 min, Stirring intensity = 100 rpm, Cell voltage = 0-15 V, Current density and Energy consumption = 1 mA/cm^2 and 1.5 kwh/kg	Na_2SO_4 (5000 mg/L)	HPLC and LC-TOFMS	Identify degradation products	Robles-Molina et al. (2012)
Nb/PbO_2 anodes and graphite carbon bar cathode	Initial COD = 450 mg/L, Temperature = 25 ºC, Electrolysis time = 10 h, Current density and Energy consumption = 50 mA/cm^2	H_2SO_4	–	COD = 76%	Samet et al. (2010a)
Boron-doped diamond (BDD) anodes and graphite carbon bar cathode	Initial COD = 450 mg/L, Temperature = 70 ºC, pH = 2, Electrolysis time = 6 h, Current density and Energy consumption = 20 mA/cm^2	H_2SO_4	–	COD = 100%	Samet et al. (2010b)

2.3 Carbofuran

Carbofuran (2,2-Dimethyl-2,3-dihydro-1-benzofuran-7-yl methylcarbamate) comes in the category of n-methyl carbamate that operates by inhibiting cholinesterase. Carbamate insecticides are used on crops and in the home to kill cockroaches, ants, fleas, crickets, etc. Carbamates are widely used pesticides and have been reported to be present in surface and ground water in the world including India. Carbofuran belongs in the category of carbamate insecticides used for the control of insects and nematodes found in most of the fruit, vegetable and agriculture crops (Salman et al., 2011). Carbofuran is a persistent carbamate insecticides compred to other carbamate or organophosphate insecticides. (Salman et al., 2010a). The mode of action of these insecticides is mostly similar to organophosphate insecticides. Degradation of carbofuran in soil takes place by hydrolysis, microbial action and to a lesser extent by photodecomposition. The persistence of carbofuran in environment is dependent upon pH, soil type, temperature, moisture content and the microbial population. Therefore the removal of carbofuran from water resources is necessary (Salman et al., 2011).

2.3.1 Environmental levels of carbofuran

2.3.1.1 Air

Carbofuran has low tendency to volatilize from moist soils or water, nor does it adsorb to suspended or sediment particles because it has low Henry's Law constant and low vapor pressure (Deuel et al., 1979). Agricultural field samples were tested in California to analyse the presence of carbofuran concentration in air and it was found that low concentrations of carbofuran was present in the air. After a 44 h sampling period carbofuran concentrations were observed from 0.03 to 0.66 $\mu g/m^3$ (Shibamoto et al., 1993).

2.3.1.2 Soil and water

Carbofuran is highly mobile in soil and surface runoff because of its high water solubility (351 mg/L at 25 ºC) and low adsorption coefficient (K_{oc} = 22). Consequently it has the potential to contaminate surfacewater, groundwater, lakes, rivers and streams (EXTOXNET, 2001). In acidic environments it is persistent, but dissipates more rapidly in more basic environments. Carbofuran concentration was detected as 3.0 µg/L in surveys conducted from 1971 to 1986 of Canadian private and municipal water supplies (HWC, 1991). A maximum carbofuran level ranging from 1 to 30 µg/L was found in the groundwater of USA (Cohen et al., 1984). Low carbofuran concentrations have been documented in water samples from Kenya (0.005−0.495 mg/L) in the farm lands whereas highest concentrations (0.198 mg/L) has been detected from Bangladesh paddy land water (Vithanage et al., 2016). The maximum concentration of carbofuran reported by the WHO in drinking water is 3 µg/L (Salman et al., 2011) and in another report it is 0.007 mg/L (WHO, 1998; Vithanage et al., 2016).

Carbofuran degrades in water by hydrolysis, photolysis and microbial decomposition. Hydrolysis half-life of carbofuran in water at 25 °C was reported as 690 days at pH levels of 5 and 6, 82 days at pH 7 and 7 days at pH levels 8 and 9, respectively (HWC, 1991; Chu et al., 2006). According to another reported data its half-life was 321 days at acidic pH 5.7 and 149 days at pH 7.7 (Pimmata et al., 2013; Fenoll et al., 2013).

2.3.1.3 Food

According to WHO, FAO and EPA carbofuran detected in treated crops is usually very low or not detectable and does not bioaccumulate in food. The half-life of carbofuran is approximatley 4 days if applied to the roots of crops, and more than 4 days when applied to the leaves of crops (FAO/WHO, 1980; US EPA, 1987).

2.3.2 Toxicity of carbofuran

Acute toxicity tests were conducted on the most sensitive life stage of fish weight from 0.5-5 grams. The LC_{50} or half maximal effective concentration (EC_{50}) are shown in Table 2.14 (DHS, 1988).

Table 2.14: Acute toxicity of carbofuran.

LC_{50} or EC_{50}	**Category description**
< 0.1 ppm	Very highly toxic
0.1 – 1 ppm	Highly toxic
> 1 < 10 ppm	Modertely toxic
> 10 < 100 ppm	Slightly toxic
> 100 ppm	Practically non-toxic

2.3.3 Effect of carbofuran

Carbofuran is highly hazardous after acute oral administration. Tests conducted on cats, guinea-pigs, rabbits, rats, dogs and mice showed toxicity levels from 3 to 19 mg/kg of body weight. It was observed that carbofuran was toxic for cholinesterase inhibition; cramps, salivation, sedation and trembling symptoms were observed within few seconds after administration. Carbofuran is neither genotoxic nor tumorigenic, but it is neurotoxic (WHO, 2001; Katsumata et al., 2005; Pimmata et al., 2013). Carbofuran poisoning was reported in workers working in agriculture fields. Signs of poisoning involved vomiting, nausea, lassitude and hypersalivation have been reported (WHO, 2004c).

Clinical symptoms, such as body weight gain, organ weight gain, significant decrease in water consumption, pathological and histopathological changes in liver and kidneys were observed. It was also observed that carbofuran had no significant effect on

haemoglobin (Hb) and total red blood cells (RBC), but total white blood cells (WBC) showed a significant decrease (Gupta, 1994; Brkic et al., 2008).

2.3.4 Guideline value of carbofuran

Chu et al. (2006) recommended maximum contamination level (MCL) for carbofuran as 7×10^{-6} mM, but carbofuran concentration was detected between 1 and 500×10^{-6} mM in different U.S. states in groundwater. Carbofuran was also frequently detected in ground water contaminants in Europe as well as Asia over the last two decades (Kladivko et al., 1991; Matthiessen et al., 1995; Angelidis et al., 1996; Loewy et al., 1999; Campbell et al., 2004).

The US EPA recommends MCL of 40 µg/L for drinking water (US EPA, 1995). California Department of Health Services (DHS) established MCL of 0.018 mg/L (DHS, 1988). The European Union (EU) has set an MCL of 0.1µg/L for an individual pesticide and 0.5 µg/L for the sum of all pesticides and in drinking water (Council Directive 98/83/EC; Lopez-Blanco et al., 2002; Makehelwala et al., 2012).

2.3.5 Uses of carbofuran

Food: Carbofuran has been recommended for use on the subsequent crops/sites: artichoke, alfalfa, barley, banana, corn, coffee, cucumber, grapes, melons, oats, plantain, pepper, potato, soybean, squash, sugarcane, sorghum, sunflower, sugar beet, and wheat. Carbofuran is widely used on soybeans, rice, potatoes, fruits and vegetables to prevent and eliminate pests and insects which cause damage to crops up to a large extent (Teerakun, 2004; Chang et al., 2014).

Non-food: Ornamental and/or shade trees, ornamental non-flowering plants, ornamental herbaceous plants, cotton, and agricultural fallow land (Bradbury, 2007) are treated to prevent pests.

2.3.6 Reaction pathway of carbofuran

The main degradation pathway of carbofuran is hydrolysis under alkaline conditions. The identified transformation products of carbofuran are - 2, 2 dimethyl-2, 3-dihydro-benzofuran-7-ol (*M*) and 2, 3-dihydro-3-keto-2, 2-dimethyl-benzofuran-7-yl methylcarbamate (*N*) (Figure 2.3). *M* further decomposed to 2, 2 dimethyl-2, 3-dihydro-benzofuran-3, 7-diol (*P*) and *N* decomposed to *P* and 2, 2-dimethyl-oxo-2, 3-dihydro-benzofuran-7-yl methylcarbamate (*Q*). Due to the hydrolysis *P* and *Q* formed 2, 3-dihydroxybenzaldehyde as an intermediate product and further convert to CO_2 (Katsumata et al., 2005; Ma and Sung, 2010; Fenoll et al., 2013).

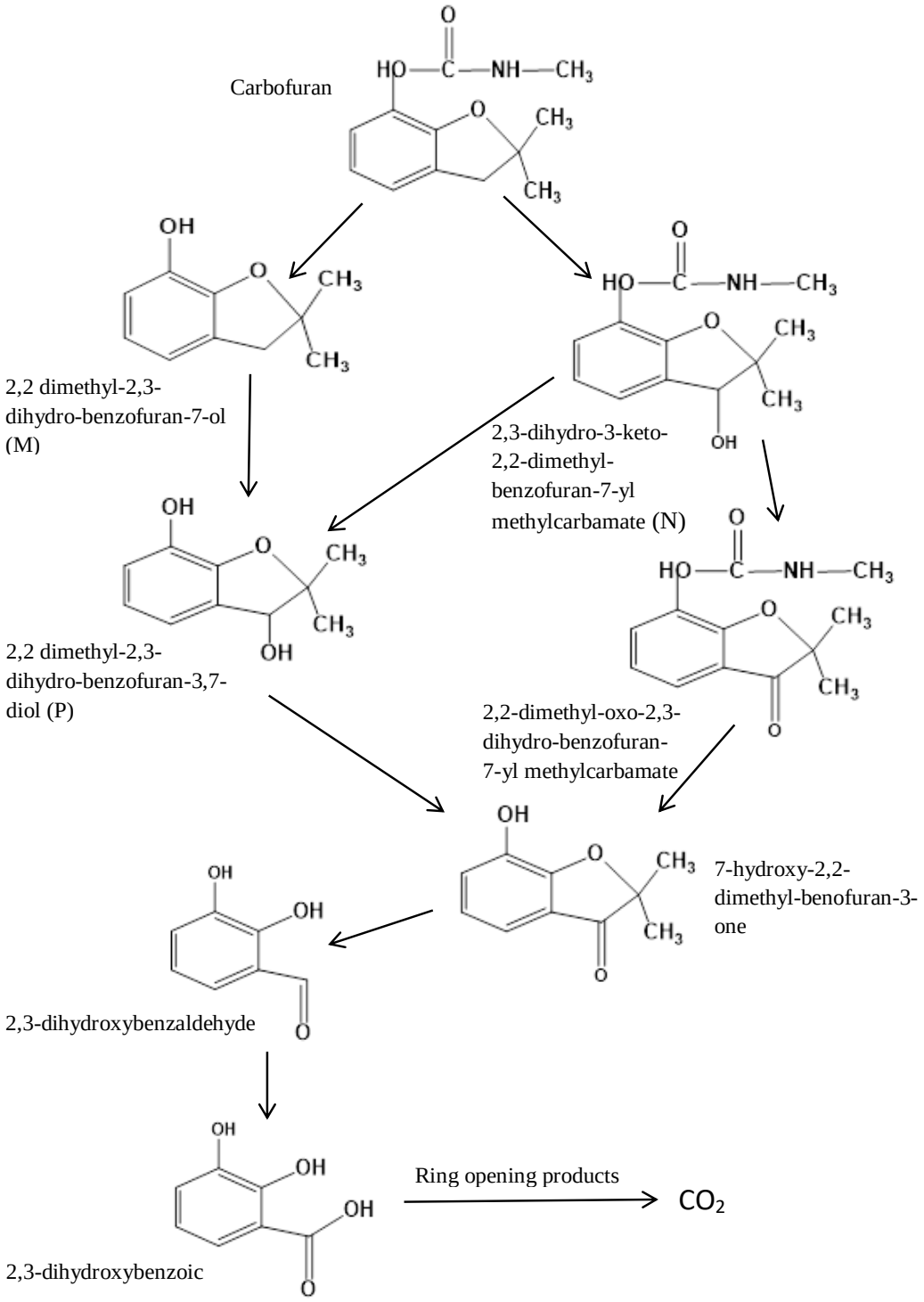

Figure 2.3: Proposed reaction pathway for carbofuran degradation.

2.3.7 Technologies used for carbofuran degradation

Available literature on degradation of chlorpyrifos using adsorption, Fenton, photo-Fenton, photocatalytic degradation and ozonation are presented in the following sections.

2.3.7.1 Adsorption

Vithanage et al. (2016) reported comparative study for carbofuran adsorption onto rice husk and tea waste derived biochars produced at 700 ºC. Adsorption studies were conducted in a batch reactor. Equilibrium adsorption capacities of rice husk biochars (RHBC) and tea waste biochars (TWBC) determined by pseudo second order kinetic model were 25.2 and 10.2 mg/g, respectively.

Chang et al. (2014) prepared activated carbon from rice straw for the removal of carbofuran from aqueous solution. The effects of various operating parameters on adsorption capacity and kinetics were observed on batch scale. The surface area and average pore diameter of the activated carbon were 1304.8 m^2/g and 2.39 nm, respectively. The optimum conditions were obtained at initial carbofuran concentration 200 mg/L, time 90 min, adsorbent loading of 100 mg/L and temperature 30 °C, on which maximum adsorption capacity occurs at 296.52 mg/g. Equilibrium adsorption isotherms were fitted better by the Langmuir model. The adsorption kinetic followed a pseudo-second-order kinetic model.

Salman et al. (2011) conducted batch adsorption studies using date seed activated carbon (DSAC). The concentrations of bentazon and carbofuran in the solutions were analyzed by double beam UV–Vis spectrophotometer before and after adsorption at maximum wavelengths of 232 nm and 276 nm, respectively. They found that with increase in the pH of initial solution the equilibrium adsorption of bentazon decreased. This is also due to the increase in electrostatic repulsion between bentazon ions and

DSAC surface. The experimental results showed no significant variation in the amount of carbofuran adsorbed with increase in the pH range 2−12. The adsorption of bentazon and carbofuran was better described by the pseudo-second order equation. The percent desorption efficiencies of 84.1 and 82.2% were obtained after three cycles of adsorbent use for bentazon and carbofuran, respectively. Maximum removal of pesticide was achieved at 90% with solution of initial concentration 100 mg/L. The results showed higher adsorption efficiency of DSAC for carbofuran than bentazon. The concentration of carbofuran can be analyzed either by HPLC or UV-Vis spectrophotometer.

Salman et al, (2010a) conducted batch adsorption studies on the removal of carbofuran and 2,4-dichlorophenoxyacetic acid (2,4-D) using commercial granular activated carbon, filtersorb 300 (GAC F300) and observed that the concentrations of pesticide solution and contact time had important role on the adsorption of 2,4-D and carbofuran onto GAC F300. Experimental results showed that the equilibrium data fit well to the Langmuir equilibrium model for 2,4-D and carbofuran in the concentration range 50–225 mg/L. The maximum amount adsorbed was found at pH 2 for both 2,4-D and carbofuran. The monolayer adsorption capacities of GAC F300 were 181.82 and 96.15 mg/g for 2,4-D and carbofuran, respectively.

Salman et al. (2010b) studied the removal of insecticide carbofuran from aqueous solutions using banana stalks activated carbon. The results showed that the equilibrium adsorption of carbofuran decreased slightly from 65.33 to 63.54 mg/g when the initial pH of the aqueous solution was increased from 2 to 12. They found that BSAC had good recoverability and reusability characteristics through regeneration by adsorption and desorption process which were repeated in three cycles. The removal of carbofuran from aqueous solution decreased from 98.4 to 85% for the first to the third cycle. This may be because of the decrease in adsorbent weight by washing and drying of sample.

The desorption was 97.5, 97.1 and 96.97% for the first, second and third cycles, respectively, were observed.

Memon et al. (2007) performed the removal of carbofuran (CF) and methyl parathion (MP) using chestnut shells as adsorbent in aqueous solution. The effects of sorption parameters, i.e., contact time, pH, initial pesticide solution concentration and temperature were studied. Adsorbent chestnut shell removed 99±1% carbofuran from aqueous solutions. Chemical treatment with nitric acid and methanol, significantly increased the sorption capacity of chestnut shells. The percentage sorption increase can be attributed to the fact that acid treatment of adsorbents may dissolve the minerals from the sorbent surface, increasing the pore volume and surface area of the sorbent.

Gupta et al. (2006) studied adsorption in batch units for abstraction of 2,4-dichlorophenoxyacetic acid (2,4-D) and carbofuran from aqueous solutions using fertilizer industry waste (carbon slurry) and steel industry wastes (blast furnace slag, dust, and sludge). They found the adsorption efficiency to vary in the order: carbon slurry > blast furnace sludge > dust > slag. Results showed that the adsorption of pesticide on carbonaceous adsorbents was a second-order process, and the maximum adsorption was about 70–80% that of the standard activated charcoal.

A Summary of the available results on the adsorption studies is presented in Table 2.15.

Table 2.15: Carbofuran removal from contaminated water by adsorption.

Adsorbents	Surface Area	Operating conditions	Optimum conditions	Adsorption capacity	Degradation	Analysis	Reference
Rice husk and tea waste derived biochars	RHBC = 342.22 m^2/g and TWBC = 377 m^2/g	Carbofuran concentration = 5-100 mg/L, biochar dose = 1 g/L Contact time = 0-700 min, pH = 5, Temperature = 25-45 °C, Agitation speed = 100 rpm	Conduct Kinetics & thermodynamics study	RHBC = 25.2 mg/g and TWBC = 10.2 mg/g	RHBC = 47.7% and TWBC = 21.5%	Double beam UV-Vis spectrophotometer at 276 nm	Vithanage et al. (2016)
Rice straw AC	1304.8 m^2/g	Carbofuran concentration = 25-200 mg/L, Contact time = 90 min, Temperature = 20-40 °C, Agitation speed = 180 rpm, pH =4.46-12.35	Carbofuran concentration = 200 mg/L, Temperature = 30 °C, Adsorbent loading = 100 mg/L	296.52 mg/g	–	–	Chang et al. (2014)
Date seed AC	BET – 880.18 m^2/g, Langmuir - 1322.24 m^2/g	Carbofuran concentration = 25-250 mg/L, Contact time = 22 h, pH = 2-12, Temperature = 30 °C, Agitation speed = 120 rpm	Carbofuran concentration = 25 mg/L, pH = 3	137.04 mg/g	90%	Double beam UV–Vis at 276 nm	Salman et al. (2011)

GAC F300	731.48 m^2/g	Carbofuran concentration = 50-225 mg/L, Contact time = 26 h, pH = 2-12, Temperature = 30 °C, Agitation speed = 120 rpm, Sorbent = 0.2 gm	pH = 2	96.15 mg/g	–	Double beam UV–Vis at 276 nm	Salman et al. (2010a)
Banana stalks AC	BET – 981.62 m^2/g, Langmuir –1466.71 m^2/g	Carbofuran concentration = 25–250 mg/L, Agitation time = 0- 13 h, pH = 2-12, Temperature = 30-50 °C, Agitation speed = 120 rpm, Sorbent = 0.3 gm	pH = 4	156.30–164.0 mg/g	96.97–97.35%	Double beam UV–Vis at 276 nm	Salman et al. (2010b)
Chestnut shells	42 m^2/g	Carbofuran concentration = (0.45–4.5) × 10^{-4} mol/dm^3, Sorbent = 0.1-1 g, Contact time = 10-100 min, pH = 6, Temperature = 373-873 K, Agitation speed = 25-150 rpm	Carbofuran concentration = 0.45 × 10^{-4} mol/dm^3, pH = 6, Agitation time = 30 min, Sorbent = 0.4 g, Temperature = 573 K, Agitation speed = 100 rpm	10.8 ± 0.3 × 10^{-6} mol/g	99 ± 1%	HPLC	Memon et al. (2007)

2.3.7.2 Photocatalytic degradation

Vishnuganth et al. (2016) used granular activated carbon supported TiO_2 (GAC-TiO_2) catalyst for photocatalytic degradation of carbofuran from aqueous solution under batch conditions. Photocatalytic degradation followed the first-order kinetics. The complete degradation (100%) of carbofuran was achieved under the optimum condition of initial concentration 50 mg/L and 100 mg/L at contact times of 90 min and 120 min, respectively.

Yang et al. (2013) reported photocatalytic degradation of carbofuran in TiO_2 aqueous solution by varying the TiO_2 loading, initial pH value and the concentration of carbofuran.

Fenoll et al. (2013) used both TiO_2 and ZnO as photocatalyst for degradation of carbofuran in leaching water. They reported that the ZnO as a better photocatalyst for the removal of carbofuran and organic intermediates.

Lopez-Alvarez et al. (2011) studied solar photocatalytic treatment of carbofuran using TiO_2 catalyst at laboratory scale as well as pilot scale, using direct sunlight. At 55 mg/L of carbofuran in a commercial formulation was eliminated after 420 min; while 80% of toxicity (1/E50 on Vibrium Fischeri), 80% of COD and 60% of dissolved organic carbon (DOC) were removed in treatment after 900 min.

Mahalakshmi et al. (2007) investigated photocatalytic degradation of carbofuran in an aqueous solution using various semiconducting materials; Degussa P-25 TiO_2 and ZnO as photocatalysts. Experiments were performed in a slurry batch reactor. The complete mineralization of carbofuran was confirmed by TOC analyzer. In all experiments cylindrical photochemical reactor of 30 cm × 3 cm (height × diameter), was provided with water circulation arrangement to maintain the temperature in the range 25–30 ºC and used mercury lamps to emit predominantly UV radiation at a wavelength of

254 nm. The effect of pH on the rate of photocatalytic degradation showed that the rate of degradation increased with increase in pH from 4 to 7 and decreased thereafter. The rate of degradation increased with increase in the carbofuran concentration. The effect of light intensity was investigated in the range 16 to 64 W. The results showed that the degradation rate increased with increase in the light intensity up to 64 W. This phenomena is due to increase in the intensity of incident light. The probability of excitation of electrons as well as the reexcitation of recombined electrons is increased. It was shown that the initial rate of degradation of carbofuran with TiO_2 is higher than that with ZnO and complete mineralization was achieved in 7h.

Chu et al. (2006) used UV/H_2O_2, UV/$S_2O_8^{2-}$, and UV/H_2O_2/$S_2O_8^{2-}$ systems to compare the treatment performances of carbofuran. System UV/H_2O_2/$S_2O_8^{2-}$ was having difficulty in breaking down the furan ring, where as the carbofuran was oxidized into carbon dioxide and so the mineralization efficiency in UV/H_2O_2/$S_2O_8^{2-}$ system was lower than the UV/$S_2O_8^{2-}$ system. UV/$S_2O_8^{2-}$ system took 30 min to remove 100% TOC whereas UV/H_2O_2/$S_2O_8^{2-}$ took 45 min.

Katsumata et al. (2005) reported photodegradation of carbofuran by excitation of iron (III) aquacomplexes under UV irradiation. Factors, such as, pH, initial concentration of Fe (III), reaction temperature and light intensity were found to affect the degradation process. An initial concentration of carbofuran of 10 mg/L was completely degraded within 50 min at pH 2.8 with original Fe (III) concentration of 8×10^{-4} mol/L.

Tennakone et al. (1997) used TiO_2 as a photocatalyst and indicated that total mineralization could be achieved after 15 h of irradiation. A 400 mL water-cooled (26 °C) photochemical reactor with a cylindrical quartz inner jacket was used for photolysis experiments. TiO_2-coated glass plates (total area 7.5×2.5 cm^2) were placed for mineralization in the carbofuran solution.

Bertrand and Barcelo (1991) used two different light sources, a Xenon arc lamp and a high-pressure mercury lamp to compare the photocatalytic behaviour on the treatment of pesticides aldicarb, carbofuran and carbaryl in distilled water, pond and artificial sea-water samples with or without humic acids. The wavelength ranges of light were between 300 and 800 nm. It was observed that wavelengths < 290 nm are the most powerful for degradation of the pesticide. In case of carbofuran it was observed that the carbofuran did not degrade with the mercury lamp (λ > 290 nm) but completely disappeared after 6 h with the unfiltered mercury lamp; whereas 11% remained after using the xenon arc lamp for 6 h. In the case of carbaryl, 35% remained after 6 h of irradiation using the filtered mercury lamp.They concluded that carbaryl was easier to degrade than aldicarb or carbofuran in distilled water. Due to the instability carbaryl can be rapidly hydrolysed in aqueous medium. The half-lives of carbofuran were observed from 60 to 90 min and from 120 to 180 min with the unfiltered mercury lamp and with the xenon arc lamp, respectively. Lower concentrations of the photoproducts were observed using the unfiltered mercury lamp than xenon arc lamp, indicating a more energetic action of the mercury lamp even on the photodegradation compounds. Only 16% of carbaryl was left after keeping a solution in pond water in the dark at 40 °C for 1 day. The results showed that photodegradation of the carbamate insecticides in distilled water using a xenon arc lamp followed the order aldicarb > carbaryl (+5% acetone) > carbaryl > carbofuran.

Results of available studies on photocatalytic degradation is summarized in Table 2.16.

Table 2.16: Carbofuran removal from contaminated water by photocatalytic degradation using different catalysts.

Catalyst	Operating conditions	Optimum conditions	Analysis	Degradation	Reference
TiO_2	Carbofuran concentration = 80 µmol/L, TiO_2 Concentration = 1.41 g/L, Temperature = room temperature, pH = 1.64-8.36, Time= 30 min, Light intensity = 0.47 mW/cm^2	Carbofuran concentration = 66.36-133.6 µmol/L, TiO_2 Concentration = 0.66-12.34 g/L, pH = 7	HPLC-MS/MS	92.85 %	Yang et al. (2013)
ZnO, TiO_2 P25 Degussa, TiO_2 anatase and TiO_2 rutile	Carbofuran concentration = 0.1 mg/L, Catalyst concentration = 0-250 mg/L, Temperature = 25±2 ◦C, pH = 6-9, Time = 0-240 min, Light intensity = UV light	Carbofuran concentration = 0.1 mg/L, ZnO Concentration = 150 mg/L, TiO_2 Concentration = 100 mg/L, pH = 8.2	HPLC	ZnO = 0.1µg/L, TiO_2 P25 Degussa = 22.4µg/L, TiO_2 anatase = 68.4 µg/L and TiO_2 rutile = 68.4µg/L	Fenoll et al. (2013)
TiO_2	Carbofuran concentration = 14–282 µmol /L, TiO_2 Concentration = 0.05-2 g/L, pH = 3-9, Time = 24 h, Light intensity = UV light	TiO_2 Concentration = 1.43 g/L, pH = 7.6, Time = 20 min	GC-MS	55 mg/L	Lopez-Alvarez et al. (2011)
TiO_2	Carbofuran concentration = 50-250 mg/L, Catalysts loading = 25-125 mg, Temperature = 24±1 ºC, pH = 4-9, Time = 0-7 h, Light intensity = 16-64 W	Carbofuran concentration = 200 mg/L, Catalysts loading = 100 mg, Temperature = 24±1 ºC, pH = 7, Light intensity = 64 W, Time = 7 h	UV-Vis/HPLC	100%	Mahalakshmi et al. (2007)

UV/H_2O_2, UV/$S_2O_8^{2-}$ and UV/H_2O_2/$S_2O_8^{2-}$	Carbofuran concentration = 0.1 mM, H_2O_2 = 1-20 mM, S_2O_8 = 0.5-20 mM, Temperature = 24±1°C, pH = 3-11, Time = 10-60 min, Light intensity = 1.5×10^{-6} mW/cm^2	H_2O_2 = 10 mM, S_2O_8 = 15 mM, pH = 7 (H_2O_2) & 3 (S_2O_8), Time = 45	LC	100%	Chu et al. (2006)
Fe(III) Aquacomplexes	Carbofuran concentration = , Fe(III) = 0-1.6×10^{-4} mol/L, Temperature = 10-40 °C, pH = 1-4, Time = 0-50 min, Light intensity = 0-2.5 mW cm^{-2}	Carbofuran concentration = 10 mg/L, Temperature = 25 °C, pH = 2.8, Time = 50 min, Light intensity = 2 mW cm^{-2}	HPLC	TOC = 70%	Katsumata et al. (2005)

2.3.7.3 Fenton oxidation and photo-Fenton

Carbofuran requires longer time for degradation, so it is recommended to use strong oxidizing agents for complete degradation in a shorter time. The carbofuran mineralization is influenced by H_2O_2 dosage rate but has little effect on DOC removal (Lu et al., 2011a).

Ying-Shiha et al. (2010) have investigated the effects of operating parameters such as dosages of H_2O_2, Fe^{2+} and initial carbofuran concentrations during carbofuran degradation by the advanced oxidation processes such as ultrasound process, Fenton process and a combined ultrasound/Fenton process. An ultrasound horn of 20 kHz was used in the experiment. They observed that more than 40% carbofuron was oxidized by ultrasonic process alone in 120 min. Combination of ultrasonic/Fenton process increased the carbofuran degradation by more than 99% and mineralization by 40% within 30 min. They found that more than 99% carbofuran was degraded by the ultrasound/Fenton process within shorter reaction time periods compared to ultrasound process and Fenton processes alone.

Summary of the results of Fenton and photo-Fenton studies is presented in Table 2.17.

Table 2.17: Carbofuran removal from contaminated water Fenton and photo-Fenton.

Method	Operating conditions	Optimum conditions	Degradation	Analysis	Reference
Photo-Fenton	Carbofuran concentration = 50 mg/L, H_2O_2 dosage = 0-6 mg/L/min, Fe dosage = 5-50 mg/L, Temperature = 25±1 °C, pH = 3, Time = 0-240 min, Light intensity = 60 μWcm^{-2}	H_2O_2 dosage = 4 mg/L/min, Fe dosage = 35 & 50 mg/L, Time = 30 min	Carbofuran = 100%, DOC = 93%	HPLC	Lu et al. (2011b)
Photo-Fenton	Carbofuran concentration = 100 mg/L, H_2O_2 dosage = 1-10 mg/L/min, Fe dosage = 1-100 mg/L, Temperature = 25±1 °C, pH = 3, Time = 0-60 min, Light intensity = 60 μWcm^{-2}	Carbofuran concentration = 100 mg/L, H_2O_2 dosage = 5.4 mg/L/min, Fe dosage = 59 mg/L, Time = 45 min	100%	HPLC	Lu et al. (2011a)
Fenton	Carbofuran concentration = 10-200 mg/L, H_2O_2 dosage = 100 mg/L, Fe dosage = 5 mg/L, Temperature = 25 °C, pH = 3, Time = 30 min	–	60%	GC–MS	Ying-Shiha et al. (2010)

2.3.7.4 Other techniques

Ozone being a powerful oxidant has been largely used as an oxidizing agent. The disadvantage of an oxidation process using ozone is that it is expensive. ***Benitez et al. (2002)*** have carried out degradation of carbofuran in batch reactor by using ozone, UV radiation and Fenton's reagent; and by the advanced oxidation processes such as combinations of ozone plus UV radiation, UV radiation plus H_2O_2, and UV radiation plus Fenton's reagent (photo-Fenton system). Degradation of carbofuran by ozone and combinations of ozone plus UV radiation was conducted at

pH 2. For all the experiments first order rate constant was used to see the efficiency of each process. It was found that the combination of ozone plus UV radiation enhanced the degradation rate of carbofuran due to the contribution of the hydroxyl radicals. In a combined O_3/UV process 90% of the carbofuran was oxidized within 50 min. Experimental results showed that the efficiency of the photo-Fenton system was much higher than the conventional ozonation and the advanced oxidation process O_3/UV.